CURRENT SCIENCE manuscript No.
(will be inserted by the editor)

Photoluminescence and Raman studies of $\alpha - MoO_3$ doped with Erbium and Neodymium

M R Joya · J E Alfonso · L C Moreno

Received: date / Accepted: date

Abstract With the objective of development optoelectronic devices, nowadays the research in this field is centered in the study of the photoluminescence emission of the rare earth elements (RE) hosted in the lattice of the different oxides. Therefore, in this work we prepared samples of Molybdenum trioxide doped with neodymium and erbium at concentrations of 1.0 % and 2.0 %, via solid state reaction technique from powders of MoO_3, Nd_2O_3 and Er_2O_3. These powders were analyzed by the X-ray diffraction (XRD) that determined the presence of phase $\alpha - MoO_3$. The morphology of the powders was made with Scanning electron microscopy (SEM), which showed that the doped samples have regular and well-defined microplates. The absorption UV-spectra revealed that the optic band gap change slightly (3.2 to 3.4 eV) with the Er, Nd, and Er-Nd concentrations. The photoluminescence shows emission bands at different wavelengths of the visible spectra as a function of the Er, Nd, and Er-Nd doped. The bands were centered at 748 nm and 808nm transitions of the Nd^{3+} ions, respectively. In this region and with excitation wavelength of 350 nm, strong emission lines were not observed for the Er. Finally, Raman spectroscopy, showed typical modes of vibration of the $\alpha - MoO_3$. Nevertheless, major changes are noted in the case of samples doped with Er, in peaks located between 350 and 580 cm^{-1}.

Keywords MoO_3 · Optical band gap · Photoluminescence · Erbium · Neodymium

M. R.Joya

Departamento de Física, Universidad Nacional de Colombia Bogotá, C.P. 111321, street 45 #30-03, Colombia
Tel.: +57 1 3165000 ext 13030
E-mail: mrinconj@unal.edu.co

J. E. Alfonso
Departamento de Física, Universidad Nacional de Colombia Bogotá, C.P. 111321, street 45 #30-03, Colombia
Grupo de ciencia de materiales y superficies

L. C. Moreno
Departamento de Química, Universidad Nacional de Colombia Bogotá, C.P. 111321, street 45 #30-03, Colombia

1 Introduction

The molybdenum trioxide ($\alpha - MoO_3$), as an intrinsic n-type II-VI semiconductor with wide bandgap ($\sim$ 3.2 eV), has been extensively utilized in organic electronics as an efficient anode with interfacial layers owing to its high work function. Moreover, the MoO_3 nanostructures have also been heavily investigated as an effective photocatalyst in pollution degradation .[1]

The molybdenum oxide (MoO_3) has been used in different applications covering electro-optic to gas sensors .[2–7] The first applications are based on the electrochromic effects that exhibit the MoO_3 .[8] This effect consists of the reversible change in transmittance and/or reflectance, caused by the application of an externally applied dc voltage and the second effect is due to a change of the electrical resistance of the oxide in the presence of gas. In recent years there have been studies which reported on the structural, optical and electrical properties of thin films of MoO_3 doped with different elements of transitions, such as Ti and nickel and/or cobalt.[3,4,7] These works focus on improving the electrochromic effect via electron transitions between two kinds of metal sites with different valences (Ti^{4+}, Ti^{3+}, Mo^{6+}, Mo^{5+}).

Moreover, the MoO_3 has been doped with rare earths such as : Er, $Er-Yb$ and Nd ions ,[5,6,8] with the objec-

tive of studying the up-conversion emission and discovering possible applications in the fields of color display, near infrared detectors, biological diagnosis, laser cooling and temperature sensors .[9–14] More recently, the MoO_3 has been used as a Hole Injection Layer (HIL) in organic light-emitting diodes (OLEDs) .[15] There are several studies of the physical-chemical properties and applications that have the MoO_3 doped and un-doped, however are few works that report the evidence of the incorporation of rare earth ions in the lattice of the MoO_3 and that explain PL [16] emission, Raman spectroscopy, UV-vis and SEM. However, the recent work by Vila *et al*,[17] is one of the few works reporting effective RE (Er and Eu) incorporation in both MoO_3 nanostructures and bulk crystals.

In the literature it is found that the photoluminescence (PL) spectra are composed of two broad peaks at 520-570 nm and 640-680 nm assigned to ($^2H_{11/2}$, $^4S_{3/2}$)$\longrightarrow$$^4I_{15/2}$ and $^4F_{9/2}$ $\longrightarrow$$^4I_{15/2}$ transitions of Er^{3+} ions, respectively .[18] For the Neodymium ion we have to the 808 nm excitation result in strong emission at 795 nm due to the $^4K_{13/2}$ $\longrightarrow$ $^4I_{13/2}$ transition along with other emissions from the Nd^{3+} ion .[19]

Therefore, in this study we presented results for the photoluminescence emission of MoO_3 as a function of Er and Nd (1.0, 2.0 %) concentrations. We also study the Raman, X-ray, SEM, UV-Vis characteristics of this material.

2 Experimental Methods

Samples of molybdenum trioxide doped with erbium and meodymium were made in atomic concentrations of 1% and 2.0% by the solid-state reaction method from Er_2O_3 (Aldrich 99.99%), Nd_2O_3 (Aldrich 99.99%) and MoO_3 (Merck 99.9%) powders. The stoichiometric amounts of oxides were mixed in isopropanol and subjected to a continuous magnetic agitation process for 8 hours, then to a drying process at a temperature of 80^o C. Finally, each sample was subjected to a calcination process for 20 hours at 550^{o}C.

The crystalline structure of these samples was characterized with a Panalytical XPert PRO X Ray difractometer (XRD) using a Bragg Brentano geometry with $Cu - k\alpha$ radiation (λ = 1.5405 $\AA$) in the 2θ range (10^o-70^o) with steps of 0.02^o). Vega3 is a thermionic emission SEM operating at 5.0 kV was used to verify the morphology of the material. Raman scattering spectra were obtained in backscattering geometry with a spectrometer JY-T64000 for samples,by using the low power Verdi 532 nm laser line excitation. The UV-vis spectrum were taken using Cary 5000 spectrometer (Varian) in diffuse reflection mode. The photoluminescence (PL) measurements were performed with a monospec 27 monochromator (Thermal Jarrel AS, USA) coupled to a R446 photomultiplier (Hamamatsu photonics, Japan). A Krypton ion laser (coherent Innova 90 K, USA) (λ=350 nm) was used as an excitation source.

3 Results and Discussion

Figure 1 shows the XRD diffraction patterns of the $Er_2O_3 - MoO_3$ and $Nd_2O_3 - MoO_3$ systems as a function of the erbium, neodymium and erbium-neodymium concentrations. Thi Figure also establishes that all crystallographic planes belong to the orthorhombic crystallographic phase of the MoO_3 (JCPDS 05-0508). In all the samples an orthorhombic crystallographic phase, is observed with the most intense peak corresponding to the plane (040) at 25.7^0 (2θ). In the XRD patterns of the molybdenum oxide mixing, with the rare earths (RE) there are no planes which belong to the oxides of RE.These results also establish that the Er^{3+} and Nd^{3+} ions are integrated at the crystallographic lattice of the MoO_3, and they will be ratified through the Raman and photoluminescence (PL) studies.

Figure 1

Powders processed for 5 h and 20 h resulted in the formation of tridimensional microplate structures with different sizes (Fig. 2 a-h). Fig. 2 (a), (d) and (g) show the micrographs of the oxides that were observed, MoO_3, Er_20_3 and Nd_2O_3, respectively. These samples are agglomerated and shapeless. Nevertheless, SEM image in fig. 2 (a) showed the presence of several irregular microplates of MoO_3 with an agglomerate nature.

Figure 2

Fig. 2 (b), (c), (e), (f) and (h) are micrographs of samples doped with Er and Nd. These micrographs show regular and well-defined microplates therefore these doped samples have very similar morphology. If we compare the figures (c) and (f) it can be observed that the doping of Er favors the growth of the grains with a more defined and regular shape. In Fig.2 (d) and (g) the micrographs of erbium and neodymium oxide are observed. These two materials do not have definite shapes in their morphology. They are simple agglomerates of material.

Figure 3

Fig. 3 show the Uv-vis spectra of MoO_3 with doped (Er and Nd) and processed by the solid-state reaction technique. Therefore, the optical band gap was determined by extrapolation of the linear portion of the curve or tail. The band gap in the materials is related to absorbance and photon energy. Therefore, the combination of absorbance and photoluminescence measurements allows the discovery of the energy levels in the materials and the optical band gap value. UV-vis measurements on the six samples showed a value of (a) 3,23 eV (MoO_3), (b) 3,25 eV (Er 1%), (c) 3,27 eV (Nd 1%), (d) 3,25 eV (Er 2%), (e) 3,26 eV(Nd 2%) and (f) 3,32 eV (Er, Nd 1%). The energy gaps are very close, however, with increasing erbium and neodymium simultaneously, the energy gap increase.

The photoluminescence (PL) property of the samples was measured at room temperature. These materials exhibit a large optical band gap of 3.05 eV, and room temperature photoluminescence at 395 nm .[25] The sample was excited with the laser line at 350 nm (3.54 eV). In fig. 4 (a) two peaks are observed at 442 nm (2.8 eV, blue) and 475 nm (2.6 eV, bluish green). The transition at 442 nm and 475 nm may be attributed to Mo^{5+} (d-d) band transition $d^2{}_{yz}$ - $d^2{}_{xz}$.[26] These emission spectra in Fig. 4 (b), exhibit a series of emission peaks with maxima at $\sim 320 - 380$ nm (UV), $\sim 410 - 480$ nm (blue), $\sim 500 - 560$ nm (green), $\sim 600 - 660$ nm (red) and $\sim 700 - 800$ nm (infrared).[27] The first major peak at 399 nm corresponds to the radiative relaxation of electrons from the lowest unoccupied molecular orbital to the highest occupied molecular orbital energy levels .[27] For Ren *etal*. [28] two ultraviolet emission bands at 344 nm and 361 nm were corresponding to the transitions of $^4D_{3/2} \longrightarrow {}^4I_{9/2}$ and $^2P_{3/2} \longrightarrow {}^4I_{11/2}$ or $^4D_{3/2} \longrightarrow {}^4I_{13/2}$. According to the energy level diagram of Nd^{3+} ion, in the literature the ion emission were found at 800 nm $^4F_{5/2}$,$^2H_{9/2} \longrightarrow {}^4I_{9/2}$ and 890 nm $^4F_{3/2} \longrightarrow {}^4I_{9/2}$.[29]

Figure 4

Fig.4 (c) shows the typical room temperature PL spectrum of Er_2O_3. The transition at 407 nm is due to the electronic transition from $^2H_{9/2} \longrightarrow {}^4I_{15/2}$, 450 nm $^4I_{15/2} \longrightarrow {}^4F_{3/2,5/2}$, 487nm $^4I_{15/2} \longrightarrow {}^4F_{7/2}$, 524 nm $^2H_{11/2} \longrightarrow {}^4I_{15/2}$, 540 nm $^2S_{3/2} \longrightarrow {}^4I_{15/2}$. In Fig.4 (c), an emission at 560 nm also appears. according to the work of Jianlan *et al*[30] it is expected to be the result of relaxation and emission from a higher energy level at an excited state of $^4S_{3/2} \longrightarrow {}^4I_{15/2}$. The peak which appears at 680 nm is possibly related to the processes relaxation from $^4F_{9/2} \longrightarrow {}^4I_{15/2}$.

Fig.4 (d) and (e) shows the PL spectra, of the Er-doped MoO_3 powders. Fig. 4 (g) and (h) shows the PL spectra of the Nd-doped MoO_3 powders. As a result of the higher the excitation energy used (350 nm) in Fig.4 (d)-(e), no emissions were observed in the range of 350 nm - 800 nm, compared to other works [31] in which the erbium-doped molybdenum trioxide was excited by a 378 nm wavelength at room temperature and heat-treated at 600^oC. Nevertheless, due to erbium doping (less 2%) the PL peaks were not observed and the material was also heat treated at 500^0C for 20 h in an air flow, a treatment equal to that of neodymium. This statement which deals with the incorporation of Er^{3+} with the material, will be confirmed with Raman spectra. Possibly, for the sample with 2% Er, the 658 nm broadband is related to defects and conceals the PL of the Er.

In Fig. 4 (g) four peaks appear at 442 nm, 751 nm, 806 nm and 818 nm with 2% Nd. The peak at 806 nm corresponds to the transition of the Nd^{3+} ion to ($^4F_{5/2}$,$^2H_{9/2} \longrightarrow {}^4I_{9/2}$ [32]). According to other works of literature ,[33,34] absorption peaks are centred at 748 nm and 808 nm which are related to the f-d transitions of Nd^{3+} internal ions in the crystal. The absorption bands are attributed to the (748 nm) $^4I_{9/2} \longrightarrow {}^4F_{7/2} + {}^4S_{3/2}$ and (808 nm) $^4G_{9/2} \longrightarrow {}^4F_{5/2} + {}^4H_{9/2}$ transition of Nd^{3+}. In our work it corresponds to the 751 nm and 806 nm peaks. The difference in peak position may be related to defects in the material. This is indicated by the presence of the neodymium in the MoO_3. A similar occurrence happens with 1% Nd, in this fig. 4 (h). Unlike erbium, changes in the photoluminescence with neodymium are more visible. For the 1% erbium and neodymium Fig. 4 (f), again very similar peaks Fig. 5(g) it appears the only difference is that the peak at 750 nm practically disappears. These small differences with the other spectra indicate that the dopant material is entering the matrix (MoO_3). In other works of literature, it is understood that it is possible to observe the PL for Er^{3+} for wavelengths of a high excitation (808 nm) .[34] However, in our study, we use wavelengths under 350 nm.

Figure5

The irreducible representation of MoO_3 with space group D_{2h} (Pb nm) is given as follows:

$$\Gamma = 8A_g + 8B_{1g} + 4B_{2g} + 4B_{3g} + 4A_u + 3B_{1u} + 7B_{2u} + 7B_{3g} \quad (1)$$

in which A_g, B_{1g}, B_{2g} and B_{3g} are Raman-active modes .[35,36] The Raman-active phonon modes can be used to estimate the structural order at a short range in the materials. A typical Raman spectrum of the $\alpha -$

MoO_3 nanoplates is shown in Fig. 5 (b). It corresponds to the atomic dispersion of an octahedron (MoO_6) in the phase $\alpha - MoO_3$. The positions of these modes can be observed in: 118 (B_2g), 129 (B_3g), 160 (Ag, B_1g), 199 (B_2g), 218 (Ag), 247 (B_3g), 285 (B_2g, B_3g), 338 (B_1g, Ag), 367 (Ag), 382 (B_1g), 472 (Ag, B_1g), 667 (B_2g, B_3g), 820 (Ag_1, B_1g) and 995 (Ag_1, B_1g) cm^{-1}.

The narrow band at 995 cm^{-1} is assignable to the antisymmetric $\nu(Mo = O_1)$ stretching .[35] The strong band at 820 cm^{-1} represents the symmetric $\nu(Mo - O_3 - Mo)$ stretching. The weak and broad bands at 667 cm^{-1} and 472 cm^{-1} are ascribable to the antisymmetric $\nu(Mo - O_2 - Mo)$ stretching (B_2g) and bending (Ag). The bands at 382 cm^{-1} and 367 cm^{-1} correspond to the $\delta(O_2 = Mo = O_2)$ scissor. The band at 338 cm^{-1} is a characteristic of the $\delta(O_3 - Mo - O_3)$ deformation. The band at 285 cm^{-1} and a weak shoulder centered at 293 cm^{-1} correspond to $\delta(O_1 = Mo = O_1)$ wagging. The bands at 247 cm^{-1} and 218 cm^{-1} correspond to the $\delta(O_2 - Mo - O_2)$ scissor .[35]

Neodymium oxide (Nd_2O_3) material has four phonons ($2A_2u$ + 2Eu) .[36] Under room temperature, three Raman bands were observed at 295 cm^{-1}, 364 cm^{-1} and 481 cm^{-1} in Fig. 5 (a). Two wide shoulders are also observed in the 637 cm^{-1} and 1076 cm^{-1} positions. The band at 481 cm^{-1} has been assigned to the A_2u mode .[30]

Fig. 5 (c), (d) corresponds to the addition of Nd 1% and 2%, respectively. In Raman spectra for concentrations of 1 an 2% (Nd^{3+}), major changes in the spectra are not observed, according to other work, it is difficult to identify vibrational modes in the fluorescent emissions that overlap the Raman spectrum in the lattice area with the 514 nm .[30] In order to excite the samples in our work, a green laser 532 nm was used. This may be a possible justification of why not many changes are observed in the Raman spectrum of MoO_3 with Neodymium doping.

Figure 6

Spectra obtained from Er_2O_3 using a 532 nm excitation are shown in Fig. 6 (a). The band at 232 cm^{-1}, 262 cm^{-1}, 381 cm^{-1}, 484 cm^{-1}, 522 cm^{-1}, 565 cm^{-1}, 606 cm^{-1}, 653 cm^{-1}, 725 cm^{-1}, 746 cm^{-1}, 831 cm^{-1}, 983 cm^{-1} and 1071 cm^{-1} corresponds to the Raman bands Er_2O_3, respectively. Fig. 6 (b) corresponds to MoO_3, and the Raman modes have already been explained in Fig. 5 (b). Fig. 6 (c), (d) corresponds to the spectra of molybdenum trioxide doped with erbium 1% and 2%, respectively. The Er^{3+} ions in the material MoO_3 induces partial amorphization of the samples as evidenced by the spectra in the region between 370 cm^{-1} and 580 cm^{-1}. The three peaks that appear in the Raman spectrum for the two erbium concentrations are wide. This is an indication that Er ions are incorporated into the material. In the case of PL this effect had not been observed. The appearance of these new peaks indicates effects in samples erbium doping. These new peaks appear at 401 cm^{-1}, 416 cm^{-1}, 456 cm^{-1}, 485 cm^{-1} and 550 cm^{-1} as shown in fig. 6. (c)-(d).

4 Conclusions

In this work, the incorporation of these ions was determined comparing the PL emission and Raman spectra of the Er and Nd oxides, with the PL emission and Raman spectra of MoO_3 doped. These measurements made with excitation line of 350 nm, evidenced a band centered at 443 nm to MoO_3 doped with Er, 806 nm to samples doped with Nd, and 803 nm in samples doped with Er-Nd, that are very different to the band of the emissions of the oxides, Which have the emission centered at 442 nm (MoO_3), and emission band between 400 and 600 nm in the neodymium and erbium oxide. These results suggest that the MoO_3 doped with the Er and Nd can be used to development middle IR optic devices. Moreover, Raman spectra excited at 532 nm, major changes in low-frequency modes with increased doping of Er were observed. Three new peaks at 400, 480 and 550 cm^{-1} are presented. These results suggest that the erbium ions be incorporated into the MoO_3 causing defects in their lattice. X-ray shows the orthorhombic phase in the samples doped. In the measurements of SEM it was observed that the doping of Er favors the growth of the grains with a more defined and regular shape.However, the gap of the samples increases with the concentration of Er and Nd compared to MoO_3.

5 Acknowledgements

The authors thank the National University of Colombia in Bogotá, We give thanks for fruitful discussions and measurements by professors Paulo De Tarso (UFC-Brazil) and Maximo Li (USP-Brazil).

6 Conflicting Interest

That we have not signed an agreement with any sponsor of the research reported in the Contribution that prevents you from publishing both positive and negative results or that forbids you from publishing this research without the prior approval of the sponsor.

References

1. Xiang D., Han C., Zhang J. and Chen W.,Gap States Assisted MoO_3 Nanobelt Photodetector with Wide Spectrum Response, Sci. Rep. 2014, **4** , 4891.
2. Ma K., Yin J., Zhang Q., Xie J., Thermal stability and photoluminescence property of hexagonal$MoO_3.0.55H_2O_4$ microrods, P.Trans. 2016,**90**,342.
3. Mahajan S.S., Mujawar S.H., Shinde P.S., InamdarbA.I. and Patilb P.S., Structural, morphological, optical and electrochromic properties of Ti-doped MoO_3 thin films,Sol. Energ. Mat. Sol. Cells, 2009,**93**,183.
4. Pereira L.G., Soledade L.E.B., Ferreira J.M., Lima S.J.G., Fernandes V.J., Araujo A.S., Paskocimas C.A., Longo E., Santos M.R.C., Souza A.G. and Santos I.M.G., Influence of doping on the preferential growth of $\alpha - MoO_3$, J. Alloys Compd. 2008,**459**,377.
5. Ren P., Liu X., Zhang K., Zhang P., Teng F., Zhang Z., Xie E. and Yan P.,Green photoluminescence from erbium-doped molybdenum trioxide Mater. Lett., 2014,**122**, 320.
6. Dong B., Li Z., Cao B., Yu N. and Sun M., Quasi-one dimensional $Er^{3+}Yb^{3+}$ codoped single-crystal MoO_3 ribbons: Synthesis, characterization and up-conversion luminescence,Opt. Commun.,2011,**284**,2528.
7. Li Z., Wang W., Zhao Z., Liu X., Song P., One-step hydrothermal preparation of Ce-doped MoO_3 nanobelts with enhanced gas sensing properties, RSC Adv.,2017, **7**,28366.
8. Alfonso J.E., Garzon R. and Moreno L.C.,Behavior of the thermal expansion coefficient of $\alpha - MoO_3$ as a function of the concentration of the Nd^{3+} ion, Phys. B:Physics of Condensed Matter. 2012,**407**, 4001.
9. Wang F., Han Y., Lim C.S., Lu Y.H., Wang J., Xu J., Chen H.Y., Zhang C., Hong M.H. and Liu X.G., Simultaneous phase and size control of upconversion nanocrystals through lanthanide doping,Nature, 2010,**463**, 1061.
10. Sun C.J., Xu Z.H., Hu B., Yi G.S., Chow G.M. and Shen J., Application of $NaYF_4 : Yb$, Er upconversion fluorescence nanocrystals for solution-processed near infrared photodetectors, Appl. Phys. Lett, 2007,**91**,191113.
11. Chatterjee D.K. , Rufaihah A.J. and Zhang Y. ,Upconversion fluorescence imaging of cells and small animals using lanthanide doped nanocrystals,Biomaterials, 2008,**29**, 937.
12. Wang G.F., Peng Q. and Li Y.D. ,Upconversion Luminescence of Monodisperse $CaF_2 : Yb^{3+}/Er^{3+}$ Nanocrystals, J. Am. Chem. Soc, 2009,**131**, 14200.
13. Garcia-Adeva A.J., Balda R. and Fernandez J. , Upconversion cooling of Er-doped low-phonon fluorescent solids, Phys. Rev. B,2009,**79**, 033110.
14. Dong B., Liu D.P., Wang X.J., Yang T., Miao S.M. and Li C.R., Optical thermometry through infrared excited green upconversion emissions in $Er^{3+}Yb^{3+}$ codoped Al_2O_3 Appl. Phys. Lett., 2007,**90** ,181117.
15. Yun J., Yang J., Hong Y. and Lee C., Low driving voltage and long lifetime organic light-emitting diodes with molybdenum oxide (MoO_3) doped hole transport layer. J. Korean Phys. Soc., 2008,**53**, 1660.
16. Rao L.S, , Rao P.V., Sharma M.V.N.V. D., Veeraiah N.,J-O parameters versus photoluminescence characteristics of $40Li_2O - 4$MO (MNb_2O_5, MoO_3 and WO_3)-$55B_2O_3$:$1Nd_2O_3$ glass systems,optik - Int. J. Lig. Elec. Opt. 2017, **142**,674
17. Vila M. , Diaz-Guerra C. , Jerez D., Lorenz K., Piqueras J. and Alves E. ; Intense luminescence emission from rare-earth-doped MoO_3 nanoplates and lamellar crystals for optoelectronic applications, J. Phys. D: Appl. Phys. 2014, **47**, 355105.
18. Dehdouh H., Bensaha R., Zergoug M., Structural modification, photoluminescence, and magnetic property enhancement with Er^{3+} doping, of solgel TiO_2 thin films, Mater. Res. Express, 2017, **4**, 086408.
19. Sukul P. P., Kumar K. (2016),Near-infrared (808 and 980nm) excited photoluminescence study in Nd-doped $Y2O3$ phosphor for bio-imaging,Methods Appl. Fluoresc. 2016,**4**, 44005.
20. Rudolph W. W., Irmerb G. , Raman spectroscopic characterization of light rare earth ions: La^{3+}, Ce^{3+}, Pr^{3+},Nd^{3+} and Sm^{3+} hydration and ion pair formation, Dalton Trans., ,2017,**46**,4235.
21. Rao M.C., Ravindranadh K., Kasturi A., and ShekhawatM.S., Structural Stoichiometry and Phase Transitions of MoO_3 Thin Films for Solid State Microbatteries, Res. J. Recent Sci.2013, **2**, 67.
22. Nagabhushana G. P., Samrat D. and Chandrappa G. T.,$\alpha - MoO_3$ nanoparticles: solution combustion synthesis, photocatalytic and electrochemical properties, RSC Adv. 2014, **4** , 56784.
23. Dagar J., Tyagi P., Ahmad R., Singh R., Sinha O. P., Sumana C. K. and Srivastava R., Application of 2D-MoO_3 nano-flakes in organic light emitting diodes: effect of semiconductor to metal transition with irradiation, RSC Adv. 2015, **5**, 8397.
24. Gillaspie D. T. , Tenent R. C. and Dillon A. C. , Metal-oxide films for electrochromic applications: present technology and future directions, J. Mater. Chem. 2010,**20**, 9585.
25. Zhao Y., Liu J., Zhou Y., Zhang Z., Xu Y., Naramoto H. and Yamamoto S., Preparation of MoO_3 nanostructures and their optical properties, J. Phys.:Condens.Matter,2003, **15**, L547.
26. Navas I., Vonodkumar R. and Pillai V.P.M.,,Self-assembly and photoluminescence of molybdenum oxide nanoparticles, Appl.Phys. A, 2011,**103** , 373.
27. Goel P. and Arora P.,Mechanism of photoluminescence enhancement and quenching in Nd_2O_3 nanoparticlesferroelectric liquid crystal nanocomposites, RSC. Adv.2015, **5**, 14974.
28. Huan R. J., Gang Z.T., Huan L.J., Juan K., Xin H. J. and Lin G.,Synthesis and photoluminescence properties of Nd_2O_3 nanoparticles modified by sodium bis(2-ethylhexyl) sulfosuccinate, Chin. Phys.B, 2008,**17**,4669.
29. Ha D.H., Kim H.J., Park J.M. and Kaewao J.,Luminescence Properties of Nd_2O_3-doped Gadolinium-Borate Glass Scintillators, New. Phys. Sae Mulli, 2015, **65**, 255.
30. Cui J. and Hopex G. A.,Raman and Fluorescence Spectroscopy of CeO_2, Er_2O_3, Nd_2O_3, Tm_2O_3, Yb_2O_3, La_2O_3, and Tb_4O_7, J.Spect. 2015,**2015**, 1
31. Zhang K., Teng F., Zhang Z. and Yan P.X., Green photoluminescence from erbium-doped molybdenum trioxide, Mater. Lett.2014, **122**, 320.
32. Tian G., Gu Z., Zhao Y. and Ma Y. ,Elimination of photon quenching by a transition layer to fabricate a quenching-shield sandwich structure for 800 nm excited upconversion luminescence of Nd^{3+}-sensitized nanoparticles.,adv. Mater. 2014,**26** ,2831.
33. Zhang M., Guo H. ,Han J , Zhang H. and Xu C., Distribution of Neodymium and properties of Nd:YAG crystal by horizontal directional solidification, J. Crys. Grow. 2012,**340**, 130.

34. Tian L., Xu Z., Zhao S., Cui Y., Liang Z., J. Zhang and X. Xu,The Upconversion Luminescence of $Er^{3+}/Yb^{3+}/Nd^{3+}$ Triply-Doped $- NaYF_4$ Nanocrystals under 808-nm Excitation, Materials. 2014, **7**, 7289.
35. Chen D., Liu M. ,Yin L., Li T., Yang Z., Li X., Fan B., Wang H.,Zhang R ,Li Z. , Xu H., Lu H., Yang D., Sun J. and Gao L. ,Single-crystalline MoO_3 nanoplates: topochemical synthesis and enhanced ethanol-sensing performance, J.Mater. Chem. 2011, **21**, 9332.
36. Windom, B. C., Sawyer, W. G., Hahn, D. W. A Raman spectroscopic study of MoS_2 and MoO_3: applications to tribological systems. Trib. Lett., 2011,**42**3, 301.

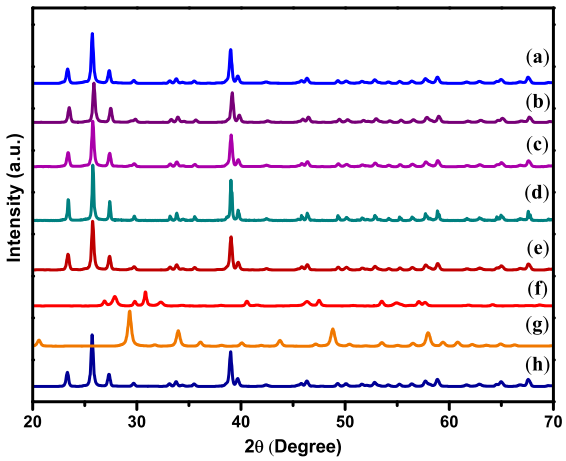

Fig. 1 (a) X-ray diffractograms of molybdenum trioxide doped with neodymium and erbium processed by the solid-state reaction method at (a) $Mo_{0.98}Nd_{0.02}O_3$, (b) $Mo_{0.98}Er_{0.02}O_3$, (c) $Mo_{0.98}Er_{0.01}Nd_{0.01}O_3$, (d) $Mo_{0.99}Nd_{0.01}O_3$ and (e) $Mo_{0.99}Er_{0.01}O_3$ 550^0C for 20 hours, (f) Nd_2O_3, (g) Er_2O_3 and (h) MoO_3 550^0C for 5 hours.

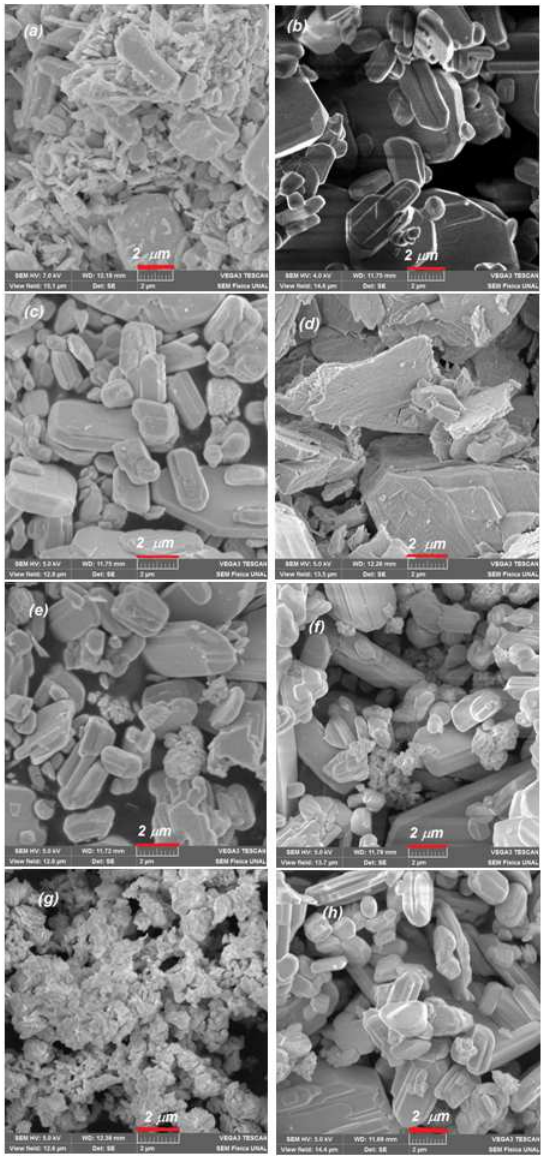

Fig. 2 SEM micrographs of molybdenum trioxide doped with neodymium and erbium processed by the solid-state reaction method at (a)MoO_3 550^0C for 5 hours, (b) $Mo_{0.99}Er_{0.01}O_3$ and (c) $Mo_{0.98}Er_{0.02}O_3$ 550^0C for 20 hours, (d) Er_2O_3 550^0C for 5 hours, (e) $Mo_{0.99}Nd_{0.01}O_3$ and (f) $Mo_{0.98}Nd_{0.02}O_3$ 550^0C for 20 hours, (g) Nd_2O_3 550^0C for 5 hours and (h) $Mo_{0.98}Er_{0.01}Nd_{0.01}O_3$ 550^0C for 20 hours .

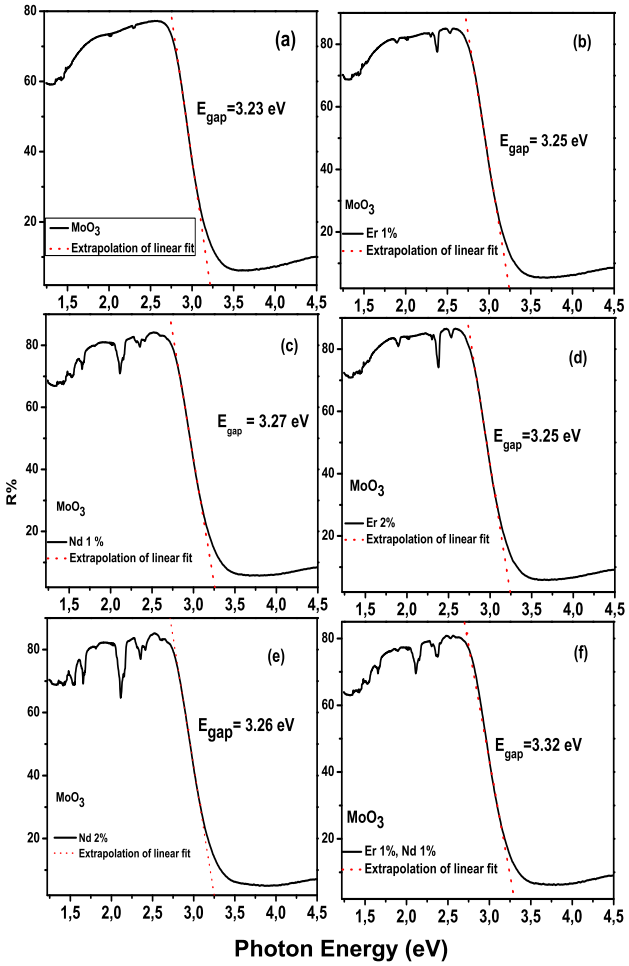

Fig. 3 UV-Vis spectra at room temperature: (a) MoO_3 550^0C for 5 hours,(b) $Mo_{0.99}Er_{0.01}O_3$, (c) $Mo_{0.99}Nd_{0.01}O_3$,(d) $Mo_{0.98}Er_{0.02}O_3$, (e) $Mo_{0.98}Nd_{0.02}O_3$ and (f) $Mo_{0.98}Er_{0.01}Nd_{0.01}O_3$ 550^0C for 20 hours.

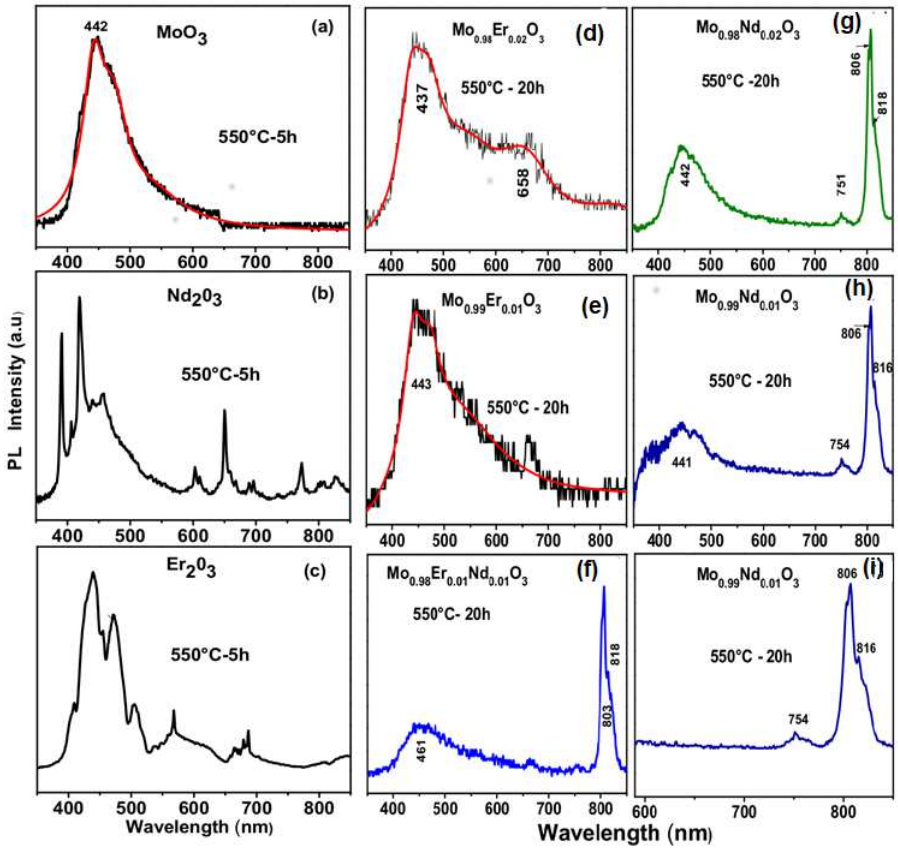

Fig. 4 Photoluminescence spectra at room temperature: (a) MoO_3, (b) Nd_2O_3 and (c) Er_2O_3 550^0C for 5 hours. In (d) $Mo_{0.98}Er_{0.02}O_3$, (e) $Mo_{0.99}Er_{0.01}O_3$, (f) $Mo_{0.98}Er_{0.01}Nd_{0.01}O_3$, (g) $Mo_{0.98}Nd_{0.02}O_3$, (h) $Mo_{0.99}Nd_{0.01}O_3$, 550^0C for 20 hours and (i) magnification of a region of the figure (h)

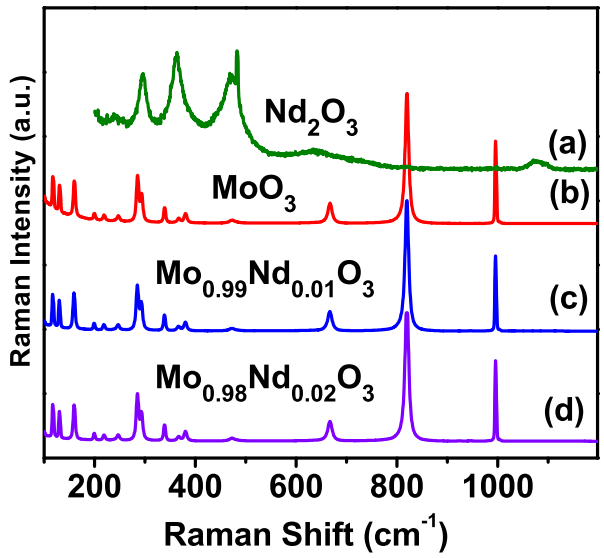

Fig. 5 Raman spectra in range from 100 to 1198 cm^{-1} at room temperature: (a) Nd_2O_3 and (b) MoO_3 550^0C for 5 hours, (c) $Mo_{0.99}Nd_{0.01}O_3$ and (d) $Mo_{0.98}Nd_{0.02}O_3$ 550^0C for 20 hours.

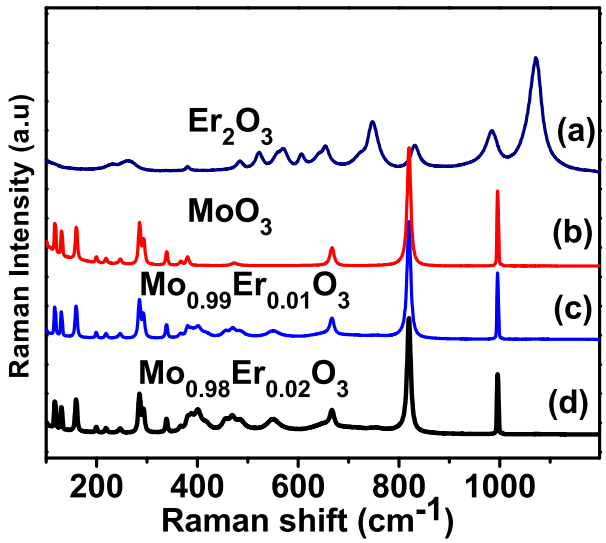

Fig. 6 Raman spectra in range from 100 to 1198 cm^{-1} at room temperature: (a)Er_2O_3 and (b)MoO_3 550^0C for 5 hours, (c)$Mo_{0.99}Er_{0.01}O_3$ and (d)$Mo_{0.98}Er_{0.02}O_3$ 550^0C for 20 hours.